Simple Mechanistic Models of Middepth Meridional Overturning

R. M. SAMELSON

College of Oceanic and Atmospheric Sciences, Oregon State University, Corvallis, Oregon

10 October 2003 and 17 March 2004

ABSTRACT

Two idealized, three-dimensional, analytical models of middepth meridional overturning in a basin with a Southern Hemisphere circumpolar connection are described. In the first, the overturning circulation can be understood as a ''pump and valve'' system, in which the wind forcing at the latitudes of the circumpolar connection is the pump and surface thermodynamic exchange at high northern latitudes is the valve. When the valve is on, the overturning circulation extends to the extreme northern latitudes of the basin, and the middepth thermocline is cold. When the valve is off, the overturning circulation is short-circuited and confined near the circumpolar connection, and the middepth thermocline is warm. The meridional overturning cell in this first model is not driven by turbulent mixing, and the subsurface circulation is adiabatic. In contrast, the pump that primarily drives the overturning cell in the second model is turbulent mixing, at low and midlatitudes, in the ocean interior. In both models, however, the depth of the midlatitude deep layer is controlled by the sill depth of the circumpolar gap. The thermocline structures in these two models are nearly indistinguishable. These models suggest that Northern Hemisphere wind and surface buoyancy forcing may influence the strength and structure of the circumpolar current in the Southern Hemisphere.

1. Introduction

In the simplest conceptualizations, the large-scale meridional overturning circulation of the World Ocean may be divided into three components: an abyssal cell associated with the northward flow of Antarctic Bottom Water and subsequent upwelling, mixing, and southward return flow; a middepth cell, involving the southward flow of upper North Atlantic Deep Water (NADW) and northward return flow of warm intermediate and upper thermocline waters; and the shallow, warm wind-driven cells associated with Ekman downwelling and subduction in the subtropical gyres. Adiabatic or weakly diffusive theoretical models of the warm wind-driven gyres and the subtropical main thermocline have been discussed by Welander (1959), Veronis (1973), Luyten et al. (1983), Samelson and Vallis (1997), and others, while the abyssal cell is likely best understood essentially as a diffusively driven circulation of the type envisioned by Stommel (1958), extended to account for spatially variable turbulent mixing (Marotzke 1997; Samelson 1998). Although large-scale numerical models routinely produce analogs of the middepth cell, simple three-dimensional analytical models for this intermediate overturning circulation have received relatively less attention.

This paper briefly describes two simple analytical models that possess middepth, ''upper-NADW-like'' meridional overturning cells. The first of these extends a previous model (Samelson 1999) of large-scale geostrophic circulation in an idealized Southern Ocean geometry to include Northern Hemisphere cooling. This extension was originally discussed by Samelson (2003), and the description here follows that discussion closely. This first model is relevant to recent ideas regarding the influence of Southern Hemisphere winds (Toggweiler and Samuels 1995) and Northern Hemisphere surface buoyancy forcing (e.g., Clark et al. 2001, and references therein) on the global meridional overturning circulation. In this model, the meridional cell is wind-driven and the ocean interior is adiabatic, as in the conceptual model proposed by Webb and Suginohara (2001). Such a circulation appears consistent with several recent large-scale observational analyses (e.g., Schmitz 1996a,b; Sloyan and Rintoul 2000, 2001a,b), which tend to indicate that upwelling through the main thermocline and the upper part of the deep thermocline is small equatorward of the subpolar gyres and the Antarctic Circumpolar Current (ACC), and that a diapycnal diffusivity $\kappa \approx 10^{-5}\ \mathrm{m^2\ s^{-1}}$ is likely sufficient to balance the observed upwelling in these regions.

Other interpretations of existing large-scale observations are also possible (e.g., Munk and Wunsch 1998; Talley 2003), which would require more interior or deep, near-boundary (Polzin et al. 1997) mixing to sustain the middepth overturning. The second model described here contains a diffusively driven middepth meridional over-

Corresponding author address: R. M. Samelson, 104 COAS Admin. Bldg., Oregon State University, Corvallis, OR 97331-5503.
E-mail: rsamelson@coas.oregonstate.edu

turning cell, consistent with this alternative view. Both models possess a thermal circumpolar analog of the ACC, which is driven only indirectly by surface wind stress.

The intent of the present note is to provide simple models of middepth meridional overturning that illustrate these two opposing conceptual viewpoints in an accessible yet quantitative manner. The specific examples examined here suggest that observations of mixing and water-mass conversion rates will likely be necessary to distinguish between these two mechanisms, as the thermocline structures that arise in the two models are not appreciably different.

2. A wind-driven model

Gill and Bryan (1971) studied the circulation in a large-scale numerical model with a circumpolar connection. Technically, their calculations were based on the primitive equations, but because of the coarse resolution, the model was effectively planetary geostrophic. The idealized basin geometry consisted of a rectangular box with vertical sidewalls, with gaps near the southern ends of the eastern and western boundaries, at which periodic boundary conditions were imposed to represent the circumpolar connection through Drake Passage in the Southern Ocean. The model circulation was found to depend strongly on the presence of the gap and the depth to which it extended.

Samelson (1999) offered a simple analytical theory for the steady, inviscid planetary geostrophic circulation in the Gill–Bryan geometry, for a specific form of wind and thermal forcing relevant to the Southern Hemisphere oceans: wind-driven upwelling south of the gap, surface heating and uniform Ekman transport northward across the gap, and downwelling at subtropical Southern Hemisphere latitudes north of the gap. Since the circumpolar connection prevented net meridional geostrophic flow across the gap at depths above the sill, the southward return flow across the gap latitudes was constrained to occur geostrophically beneath the sill, where it was cooled by convection as it crossed the gap latitudes. As a consequence of the thermal structure induced by this combination of Ekman transport, surface heating, and basin geometry, a thermal circumpolar current developed, whose transport depended on the imposed surface thermal gradients and the gap geometry, but not on the strength of the wind forcing. The thermal character of this current was consistent with that of the current found by Gill and Bryan (1971) in their numerical solutions. However, the thermal and wind forcing imposed north of the circumpolar connection in the model of Samelson (1999) was extremely simple, consisting of a uniform surface temperature at all latitudes north of the gap, and an effective zonal wind stress that was constant immediately north of the gap, decreased smoothly to zero in the southern subtropics, and remained zero at all points farther north. This differed substantially from the wind stress and surface buoyancy forcing to which the modern global ocean is subjected at latitudes north of the ACC.

Samelson (2003) explored the consequences of extending the analytical model of Samelson (1999) to include a simple representation of observed cooling at extreme northern latitudes, by imposing a fixed rate of conversion of warm fluid to cold fluid in the northern subpolar gyre. The details of precisely how and where the conversion takes place were purposely not specified. The inclusion of surface cooling and deep-water formation at the extreme northern latitudes resulted in a wind-driven middepth meridional overturning cell that extended across the equator, from high southern to high northern latitudes. This theory provides an accessible example of one possible mechanical model of the middepth cell associated with the formation and circulation of upper North Atlantic Deep Water. The corresponding analytical solutions for the geostrophic interior pressure and layer thickness fields are a straightforward extension of those of Samelson (1999), but, since they did not appear in Samelson (2003), are given here briefly for reference:

Surface pressure $p_s(x, y)$ south of gap ($y_s < y < y_1 = y_s + \Delta y$):

$$p_s(x, y) = -W_1 \frac{f^2}{\beta}(1 - x) \sin\left[\frac{\pi(y - y_s)}{\Delta y}\right],$$

$$W_1 = \frac{\pi V_1}{2\Delta y}. \tag{2.1}$$

Pressure $p(y, z)$ in zonal current through southern portion of gap ($y_1 < y < y_p = y_1 + \Delta y/4$):

$$p(y, z) = T_s(y)(z - H). \tag{2.2}$$

Pressure $p(y, z)$ in zonal current through northern portion of gap ($y_p < y < y_2$):

$$p(y, z) = T_s(y_p)(z + H), \quad -H < z < -h_{1e}, \tag{2.3}$$

$$p(y, z) = T_s(y_p)(H - h_{1e}) + T_s(y)(z + h_{1e}), \quad -h_{1e} < z < 0. \tag{2.4}$$

Upper-layer thickness $h_1(x, y)$ in Southern Hemisphere subtropical gyre north of gap ($y_m = y_2 + \Delta y/2 < y < y_n = y_m + \Delta y$):

$$h_1(x, y) = [h_{1e}^2 + D_0^2(x, y)]^{1/2}, \tag{2.5}$$

$$D_0^2(x, y) = \frac{2f^2}{T_2\beta} W_1(1 - x) \sin\left[\frac{\pi(y - y_m)}{\Delta y}\right]. \tag{2.6}$$

In the dimensionless equations (2.1)–(2.6), V_1 is the (constant) Ekman transport per unit longitude across the gap, $T_s(y) = T_1 + (T_2 - T_1)(y - y_1)/(y_2 - y_1)$ is the imposed surface temperature across the gap latitudes, H is the sill depth, h_{1e} is the depth of the upper layer at

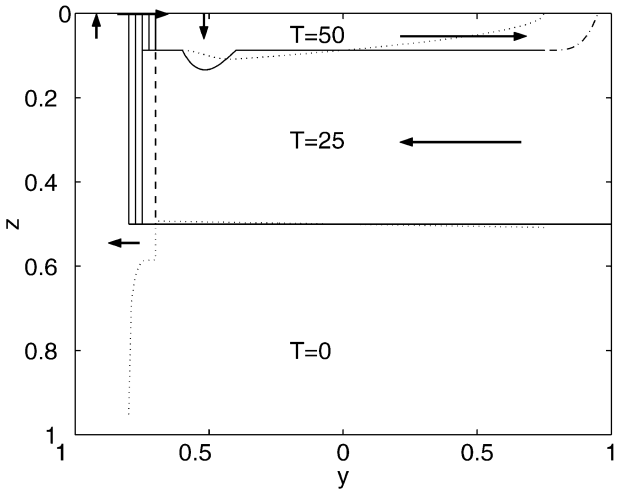

FIG. 1. Thermocline structure for the wind-driven model with Northern Hemisphere cooling (''valve on''). Temperature T is shown vs latitude y and depth z at $x = 0.5$ (solid contours) and at the western boundary (dotted contours). In the gap region, the constant meridional temperature gradients associated with the circumpolar current (2.2)–(2.4) are indicated by vertical contours at $T = \{0, 12.5, 25, 37.5, 50\}$; north of the gap, the contours indicate the interfaces between the layers $T = \{0, 25, 50\}$ at $x = 0.5$. The lateral boundaries of the basin are at $x = 0$, $x = 1$, $y = -1$, and $y = 1$, the equator is located at $y = 0$, and the gap occupies the region $y_2 = -0.8 < y < y_1 = -0.7$, $-H = -0.5 < z < 0$ (dashed contour). Meridional circulation (by surface Ekman transport and in western boundary currents) and vertical Ekman pumping and suction, are indicated (arrows). The upper interface is indicated schematically (dash–dotted line) in the subpolar gyre. After Samelson (2003).

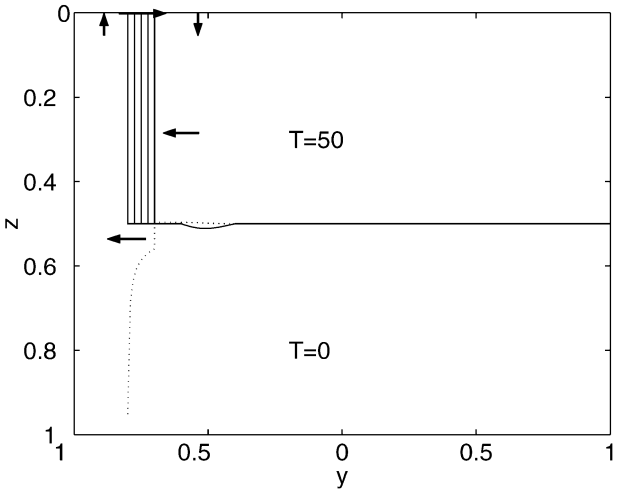

FIG. 2. Temperature T vs latitude y and depth z at $x = 0.5$ as in Fig. 1, but without Northern Hemisphere cooling (''valve off''). North of the gap, the contours indicate the interfaces between the layers $T = 0$ and $T = 50$, and the meridional and Ekman vertical circulations are indicated (arrows). After Samelson (1999).

the eastern boundary, and $f = f_0 + \beta y$ is the Coriolis parameter. [In (3.4) of Samelson (1999), y_m should appear instead of y_2, as in (2.6) above.] Note that the geostrophic-zonal current $u = -f^{-1}p_y$ in the gap depends only on the thermal and geometrical parameters, and not on the effective wind-forcing V_1. The western-boundary current transports necessary to close the circulation can be computed following Samelson (1999) and the description below of the meridional flow.

The mechanism that controls the overturning in this model may be thought of as a ''pump and valve'' system (Samelson 2003). The Ekman transport northward across the circumpolar gap acts as a pump that forces the fluid up the surface dynamic pressure gradient across the circumpolar current. The imposed conversion of warm fluid to cold fluid in the northern subpolar gyre acts as a valve that controls the flux out of the warm layer, where the surface dynamic pressure is maximum. When the valve is on (Fig. 1), the warm-to-cold conversion rate balances the northward Ekman transport, and the fluid is cold and the surface dynamic pressure is low in the Northern Hemisphere subpolar gyre. In this case, a cross-equatorial overturning cell exists, with southward return flow of cold deep water. North of the Southern Hemisphere subtropical gyre, where the northward cross-gap Ekman transport downwells, all of the meridional transport in this model is carried by western-boundary currents, both in the warm upper layer and in the cold deep layer. Continuity of boundary currents and pressure gradients across the equator is assumed. When the valve is off (Fig. 2), the model reverts to the original configuration of Samelson (1999): there is no warm-to-cold conversion at high northern latitudes, the basin north of the gap fills with warm fluid until it reaches the sill depth, and the overturning cell is short-circuited in the Southern Hemisphere, with no motion north of the Ekman downwelling latitudes of the Southern Hemisphere subtropical gyre. Note that the valve-off Southern Hemisphere overturning cell still involves water-mass conversions in the Ekman layer and in the deep-boundary current along the sill as the fluid crosses the gap [and so differs from the adiabatic Deacon cell studied, e.g., by Döös (1994) with a related layer model]; however, these conversions balance locally in zonal and vertical average, so that there is no net meridional heat transport by the cell and (like the adiabatic Deacon cell) there will evidently be no signature of the zonally averaged cell in isothermal (isopycnal) coordinates.

With northern cooling, the southward return flow occurs in the western-boundary current of the intermediate layer, which (as for the warm layer with the valve off) must deepen to the sill depth in order to support the southward geostrophic return flow across the gap. As in Samelson (1999), meridional geostrophic flow below the sill is unobstructed, and the undisturbed deep basin will fill with cold fluid up to the sill depth. Thus, in this model the sill sets the eastern-boundary depth of the intermediate layer. In the solutions discussed here, the northern warm-to-cold conversion temperature was chosen so that the fluid is cooled in the Northern Hemisphere by half the difference between the surface temperatures north and south of the Southern Hemisphere

gap. With the nondimensionalization as in Samelson (1999), the minimum temperature was $T = 0$, the maximum temperature was $T = 50$, and the warm fluid was cooled to $T = 25$ at the extreme northern latitudes of the Northern Hemisphere basin. The fluid in the deep return flow beneath the sill is colder than the surface fluid until it reaches the central latitude of the gap (where the surface temperature is $T_s = 25$), and thus does not induce convective exchange until it reaches this central latitude. Consequently, the structure of the thermal circumpolar current is no longer determined by the convective adjustment process north of this central latitude, as it is in Samelson (1999), and additional assumptions or dynamics are necessary to obtain a unique solution. One choice is to extend the surface temperatures in this region downward to the depth reached by the warm layer on the north side of the gap (Fig. 1). Alternatively, the intermediate-layer ($T = 25$) fluid could be extended upward all the way to the surface. In any case, it is interesting to note that, in this model, Northern-Hemisphere cooling has a direct effect on the strength and structure of the circumpolar current.

The depth of the warm layer north of the gap must also be determined, since it is not simply related to the sill depth as in Samelson (1999). A simple and reasonable constraint that achieves this is to choose the eastern-boundary depth of the warm layer just large enough to support northward flow in the western-boundary current from the subtropical to the subpolar gyre in the Northern Hemisphere, with volume flux equal to the northward Ekman transport at the northern edge of the Southern Hemisphere gap. This completes the warm-to-cold pathway of the meridional cell; without this flow, the warm source water would not reach the subpolar gyre, and the warm layer would again deepen as the warm fluid accumulated north of the gap. The depth of the interface on the inshore edge of the western-boundary current can be calculated from this constraint, if the warm layer is assumed to outcrop at the inshore edge of the boundary current at the subtropical–subpolar gyre boundary (Fig. 1). Because both layers are in motion in the western-boundary current, the net meridional geostrophic transport in each layer is not simply proportional to the differences in the squares of the layer depths at the eastern and western boundaries as in Samelson (1999); to complete the analytical model, some additional specification of the horizontal structure of the geostrophic boundary currents would be necessary. It is interesting to note that the inclusion of wind stress forcing in the Northern Hemisphere would presumably cause an additional increase in the eastern-boundary depth of the warm layer, to support geostrophic return flow of the southward Ekman transport out of the subpolar gyre (e.g., Samelson and Vallis 1997). Under the present assumptions, this would also influence the strength and structure of the circumpolar current in the Southern Hemisphere.

In summary, the meridional circulation cell in this model consists of wind-driven upwelling south of the gap ($y < -0.8$ in Fig. 1), northward surface Ekman transport across the gap to the subpolar–subtropical gyre boundary ($y = -0.6$), Ekman downwelling into the warm ($T = 50$) layer in the subtropical gyre ($-0.6 < y < -0.4$), and northward western boundary current transport from the Southern Hemisphere subtropical gyre to the Northern Hemisphere subtropical–subpolar gyre boundary ($y = 0.75$), followed by cooling and sinking into the intermediate ($T = 25$) layer in the northern subpolar gyre, and southward intermediate-layer return flow in the western boundary current to the gap and then across the gap beneath the sill.

One point to be made with this model is that an analog of the NADW meridional overturning cell can be constructed in which there is no interior mixing at all: all the thermodynamic exchange occurs where the fluid is exposed to the surface forcing at high latitudes. Of course, it should be borne in mind that this model contains a number of fundamental idealizations and simplifications. For example, mesoscale eddy processes in the Southern Ocean, which have been purposely neglected, could compensate much of the Ekman transport across the ACC (e.g., Marshall and Radko 2003) and alter the large-scale heat and momentum balances, while observations (e.g., Speer et al. 2000) suggest that some of the southward NADW flow and subsequent upwelling into the ACC may occur above the levels at which topography can support southward geostrophic flow. Substantial thermohaline transformations clearly do occur in the deeper part of the NADW cell, associated in part with the diffusively driven abyssal AABW cell; such interior mixing processes have also been purposely neglected in the present model.

The model has a number of appealing aspects, at least for pedagogical purposes. It provides an explicit analytical formulation of a conceptual model of one variety of overturning circulation that has been developed to varying degrees by previous authors (e.g., Toggweiler and Samuels 1995; Webb and Suginohara 2001; Nof 2003). A shutdown, or short-circuiting, of the meridional overturning cell is indicated by this steady model when the valve is switched from on to off; such a shutdown of meridional over-turning by the analogous introduction of a freshwater cap in the Northern Hemisphere subpolar gyre has been previously found and studied in numerical models (e.g., Stocker and Wright 1991). Unlike the circulation considered by Samelson (1999), the present model supports a northward ocean heat flux representative of that associated with the observed NADW cell (e.g., Talley 2003), with surface heating at the gap latitudes in the Southern Hemisphere and surface cooling in the subpolar gyre of the Northern Hemisphere. Note also that since all of the meridional transport in the intermediate layer ($T = 25$) occurs in the western-boundary currents, the intermediate layer is at rest in the interior, and it would be straightforward to supplement this analytical model with additional

warmer fluid layers representing a subtropical ventilated thermocline (Luyten et al. 1983) and its equatorial extensions (e.g., Pedlosky and Samelson 1989). It may be possible to explore some aspects of Antarctic Mode and Intermediate Water formation and circulation within the resulting framework, as the present warm-layer circulation may prove to be most closely related to these. A surprising implication of this model is that the Northern Hemisphere wind stress and deep-water formation may affect the strength of the circumpolar current; this is an intriguing counterpoint to the recent suggestion (Toggweiler and Samuels 1995) that Southern Hemisphere winds may control the Northern Hemisphere deep-water formation rate.

3. A diffusively driven model

The relation between middepth meridional overturning and small-scale mixing in the ocean remains poorly understood. Observations in the main thermocline suggest that that mixing rates correspond to turbulent diffusivities of order 10^{-5} m^2 s^{-1}. Several recent large-scale observational analyses (e.g., Schmitz 1996a,b; Sloyan and Rintoul 2000, 2001a,b) indicate that upwelling through the main thermocline and the upper part of the deep thermocline is small equatorward of the subpolar gyres and the ACC, and that $\kappa \approx 10^{-5}$ m^2 s^{-1} is likely sufficient to balance the observed upwelling in these regions Webb and Suginohara (2001). This point of view is consistent with the wind-driven overturning model discussed in the previous section.

On the other hand, the quantitative constraints on large-scale budget analyses remain relatively weak, and other interpretations are possible (Munk 1966; Munk and Wunsch 1998). Talley's (2003) analysis provides a particularly striking example of this: in a global meridional transport section at 32°S, the middepth cell corresponding to northward transport of warm thermocline water and southward transport of cold upper NADW does not appear (Talley 2003, her Fig. 7). The implication of this result is that the cold-to-warm conversion that balances the 20 Sv (1 Sv $\equiv 10^6$ m^3 s^{-1}) warm-to-cold conversion and NADW production in the North Atlantic (Talley 2003, her Fig. 6a) in this cell must occur north of 32°S (mostly in the Pacific and Indian Oceans, presumably). Since the corresponding isopycnals are isolated from surface forcing north of 32°S, except in regions of surface cooling, this cold-to-warm conversion requires turbulent mixing in the ocean interior or near the bottom boundary. If this picture is correct, then this part of the NADW overturning cell must be driven by turbulent diffusion, not by Ekman transport across the ACC. The implied turbulent diffusivities in this case will be larger than the canonical 10^{-5} m^2 s^{-1} interior ocean values.

This alternative point of view is not consistent with the wind-driven overturning model discussed in the previous section. A calculation that may be more relevant to this point of view is discussed by Samelson (1998), who described the circulation that developed in a single-basin, planetary geostrophic numerical model, when the turbulent vertical heat diffusivity was taken to be large along the eastern boundary of the basin. In this eastern-boundary mixing region, the vertical divergence of vertical heat diffusion was balanced by vertical advection, with large vertical velocities at middepth. A Sverdrup vorticity balance still obtained in the eastern-boundary region, so that the warm fluid above middepth moved equatorward, while the cold fluid below middepth moved poleward. In order to close the circulation, the warm near-surface fluid flowed zonally out of the eastern boundary region to the western boundary, and then meridionally to the subpolar gyre, where it cooled and sank. The cold, deep, subpolar fluid flowed back into the western boundary layer and then meridionally to subtropical latitudes, where it then flowed eastward to the eastern boundary mixing region.

A similar circulation can be introduced into the present model in a simple way. The cold-to-warm water-mass transformation induced by the enhanced mixing may be represented in the layer model by a specified flux of cold-layer fluid into the warm layer. This transformation may be imposed, for example, over the eastern half of the Southern Hemisphere subtropical gyre. This distribution of mixing may be considered as a crude representation of the observations of Polzin et al. (1997). For the present calculation, the cold-to-warm flux w_δ is specified as

$$w_\delta(x, y) = w_0 \sin^2\left[\frac{(y_2 - y)\pi}{(y_2 - y_\delta)}\right], \qquad x_\delta \le x < x_E, \qquad y_\delta \le y < y_2, \quad (3.1)$$

where the subscript E indicates the eastern boundary value, and $w_\delta = 0$ elsewhere. If there is no mechanical forcing in the mixing region, the Sverdrup relation reduces to

$$H_2^2 + \Gamma H_1^2 = H_{2E}^2 + \Gamma H_{1E}^2, \quad (3.2)$$

where H_j is the depth of the interface at the base of layer j, $j = 1$ or 2, and $\Gamma = \gamma_1/\gamma_2$, with γ_j the corresponding reduced gravities. Since the layer-2 thickness $h_2 = H_2 - H_1$, it follows from the layer-2 vorticity balance, $\beta h_2 v_2 = f w_\delta$, that

$$a^2 H_2^2 - \Gamma^{-1/2}\left\{\arcsin(aH_2) + \frac{1}{2}\sin[2\arcsin(aH_2)]\right\} = a^2 H_{2E}^2 - \Gamma^{-1/2}\left\{\arcsin(aH_{2E}) + \frac{1}{2}\sin[2\arcsin(aH_{2E})]\right\} + \frac{2a^2 f^2}{\beta\gamma_2}\int_{x_E}^{x} w_\delta\, dx', \quad (3.3)$$

where

$$a = (H_{2E}^2 + \Gamma H_{1E}^2)^{-1/2}. \quad (3.4)$$

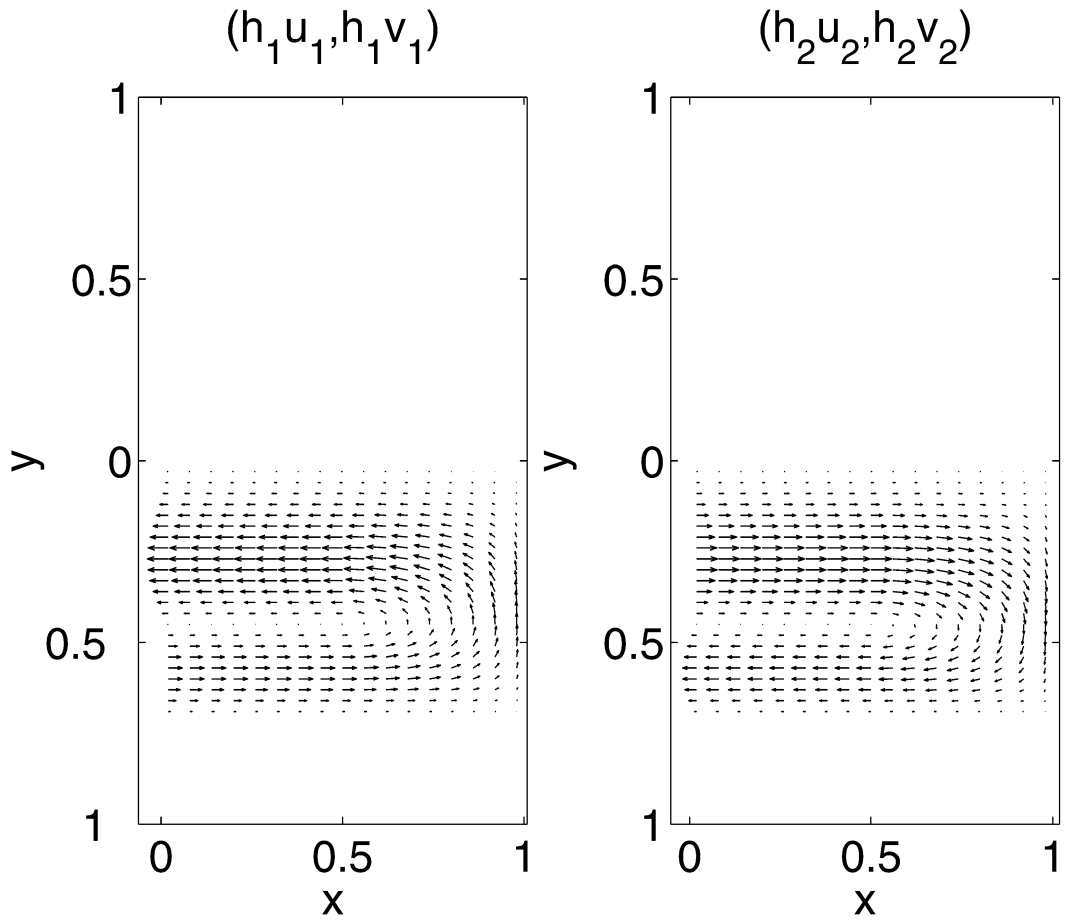

FIG. 3. Transport vectors in the (left) upper and (right) lower layers for the circulation driven by the interfacial mass flux w_δ from (3.1), with $w_0 = 4$, $x_\delta = 0.5$, and $y_2 = -0.7$.

Equation (3.3) may then be solved numerically for $H_2(x, y)$, after which $H_1(x, y)$ can be obtained from (3.2). For $x < x_\delta$ and $y_\delta \le y < y_2$, $h_j(x, y) = h_j(x_\delta, y)$, $j = 1, 2$, and elsewhere the interface depths are constant and equal to their eastern boundary values.

With this representation of interior mixing, poleward Sverdrup flow results in the cold, lower layer in the mixing region, and equatorward Sverdrup flow in the warm, upper layer (Fig. 3). The associated warm-layer convergence and cold-layer divergence on the equatorial side of the gyre is balanced by zonal flow to the western boundary. The warm fluid that arrives at the western boundary may then flow in the western boundary current to high northern latitudes, where it cools and sinks. The resulting cold deep water returns southward in a deep western boundary current, completing the overturning cell.

Suppose now that the wind-forcing across the circumpolar gap is weak, so that the wind-driven meridional overturning cell is also weak. Alternatively, suppose that most of the northward Ekman transport across the circumpolar gap is balanced locally by southward eddy fluxes, as in the model of Marshall and Radko (2003). In either case, the weak northward transport will still result in a deep return flow at the sill depth and a thermal circumpolar current, as argued by Samelson (1999), but the motion and interface deformation north of the gap will be negligible. North of the gap, then, the flow and interface deformation may be accurately approximated by the diffusively driven solution (3.3). As in the wind-driven model, H_{2E} must equal the sill depth at the gap, in order to support the deep geostrophic return flow. Similarly, a reasonable choice for H_{1E} is the minimum depth that will support the required northward transport of warm water into the Northern Hemisphere subpolar gyre in a geostrophic boundary current, where the total northward flux of warm water is obtained from the area integral of the specified upwelling velocity (3.1).

The resulting thermocline structure (Fig. 4) is very similar to the wind-driven case (Fig. 1). The only qualitative difference is the upward deformation of the deep interface at the Southern Hemisphere mixing latitudes. For particular choices of parameters, there may be differences in the structure and extent of the anticyclonic circulation in the Southern Hemisphere warm layer, and

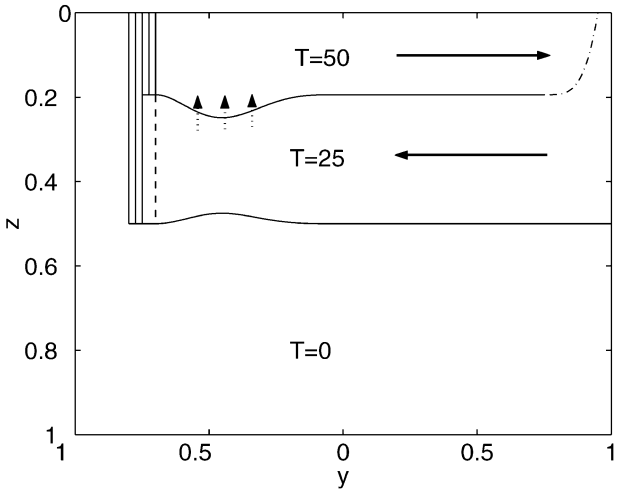

FIG. 4. As in Fig. 1, but for the diffusively driven (and weakly wind-driven) model, with interfacial mass flux parameters as in Fig. 3. The diffusively driven interior flux of cold-layer fluid into the warm layer (dotted arrows) and the associated meridional transport in western boundary currents (solid arrows) are indicated. (Meridional and vertical transports associated with the weak wind-driven cell across the circumpolar gap are not indicated.) The upper interface is indicated schematically (dash–dotted line) in the subpolar gyre.

in the eastern boundary depth H_{1E} required to support cross-gyre transport into the Northern Hemisphere cooling region. Note that no downward Ekman pumping is required to support the Southern Hemisphere anticyclonic gyre, which is driven by the upward mass flux w_δ across the upper interface. In principle, this upward mass flux could be imposed anywhere in the subtropical regions north of the gap; for the particular solution discussed here, it was restricted, for simplicity, to the Southern Hemisphere. If it were confined to regions small relative to eddy-viscous boundary layer widths, the interior recirculations would be weakened (e.g., Spall 2000), and the distinction in the two interior thermocline structures would be further reduced.

4. Summary

Two simple models of large-scale middepth overturning have been discussed here. In both, the meridional overturning cell involves upwelling and warming of cold fluid in the Southern Hemisphere, transport of warm Southern Hemisphere fluid to high northern latitudes in western boundary currents, cooling and sinking at high northern latitudes, and return flow of cold Northern Hemisphere fluid to the Southern Hemisphere in deep western boundary currents. The models differed primarily in their mechanisms for upwelling and warming of cold Southern Hemisphere fluid. In the first model, the upwelling was driven by Ekman suction in a cyclonic subpolar gyre south of the circumpolar gap, followed by northward Ekman transport across the gap. In the second model, the upwelling was presumed to be driven by subsurface turbulent mixing, also in the Southern Hemisphere, but north of the gap. Despite these fundamental differences in the forcing mechanisms in these two models, the resulting thermocline structures are almost identical. Part of this similarity arises because the depth of the midlatitude deep layer is set in both models by the sill depth of the circumpolar gap. These models suggest that Northern Hemisphere wind and surface buoyancy forcing may influence the strength and structure of the circumpolar current in the Southern Hemisphere.

In each case, the warm fluid in the middepth meridional overturning cell was presumed to flow preferentially in geostrophic boundary currents down the pressure gradient to high northern latitudes, rather than ageostrophically (through eddy fluxes) across the thermal current that developed in the circumpolar gap. A more complete theory would include, along with a concrete dynamical representation of the northern cooling and sinking region, a more explicit consideration of the competition between the two paths that return warm water to high latitudes: southward through the interior and across the gap by ageostrophic eddy processes, and northward along the basin edges in geostrophic boundary currents. In large-scale numerical ocean circulation models, this competition must evidently involve a balance between parameterized eddy processes in the ACC and parameterized frictional processes in western boundary currents. This apparently unavoidable balance of parameterizations would appear to present a severe challenge to numerical modeling and prediction of the middepth meridional overturning circulation.

Acknowledgments. This research was supported by the National Science Foundation, Grant OCE-9907854, and the Office of Naval Research, Grant N00014-98-1-0813. I am grateful for conversations with B. Sloyan, K. Speer, and L. Talley, and for the constructive comments of three anonymous reviewers.

REFERENCES

Clark, P., N. Pisias, T. Stocker, and A. Weaver, 2001: The role of the thermohaline circulation in abrupt climate change. *Nature*, **415,** 863–869.

Döös, K., 1994: Semi-analytical simulation of the meridional cells in the Southern Ocean. *J. Phys. Oceanogr.*, **24,** 1281–1293.

Gill, A., and F. Bryan, 1971: Effects of geometry on the circulation of a three-dimensional Southern Hemisphere ocean model. *Deep-Sea Res.*, **18,** 685–721.

Luyten, J., J. Pedlosky, and H. Stommel, 1983: The ventilated thermocline. *J. Phys. Oceanogr.*, **13,** 292–309.

Marotzke, J., 1997: Boundary mixing and the dynamics of three-dimensional thermohaline circulations. *J. Phys. Oceanogr.*, **27,** 1713–1728.

Marshall, J., and T. Radko, 2003: Residual-mean solutions for the Antarctic Circumpolar Current and its associated overturning circulation. *J. Phys. Oceanogr.*, **33,** 2341–2354.

Munk, W., 1966: Abyssal recipes. *Deep-Sea Res.*, **13,** 707–730.

——, and C. Wunsch, 1998: Abyssal recipes II: Energetics of tidal and wind mixing. *Deep-Sea Res.*, **45A,** 1977–2010.

Nof, D., 2003: The Southern Ocean's grip on the northward merid-

ional flow. *Progress in Oceanography,* Vol. 56, Pergamon, 223–247.

Pedlosky, J., and R. Samelson, 1989: Wind forcing and the zonal structure of the Equatorial Undercurrent. *J. Phys. Oceanogr.,* **19,** 1244–1254.

Polzin, K., J. Toole, J. Ledwell, and R. Schmitt, 1997: Spatial variability of turbulent mixing in the abyssal ocean. *Science,* **276,** 93–96.

Samelson, R. M., 1998: Large-scale circulation with locally enhanced vertical mixing. *J. Phys. Oceanogr.,* **28,** 712–726.

——, 1999: Geostrophic circulation in a rectangular basin with a circumpolar connection. *J. Phys. Oceanogr.,* **29,** 3175–3184.

——, 2003: Meridional overturning as a ''pump and valve'' system. *Near-Boundary Processes and Their Parameterization: Proc. 'Aha Huliko'a Hawaiian Winter Workshop,* Honolulu, HI, University of Hawaii at Manoa, 205–209.

——, and G. K. Vallis, 1997: Large-scale circulation with small diapycnal diffusion: The two-thermocline limit. *J. Mar. Res.,* **55,** 223–275.

Schmitz, W. J., Jr., 1996a: On the World Ocean circulation: Volume I. Woods Hole Oceanographic Institution Tech. Rep. WHOI-96-03, 141 pp.

——, 1996b: On the World Ocean circulation: Volume II. Woods Hole Oceanographic Institution Tech. Rep. WHOI-96-08, 237 pp.

Sloyan, B., and S. Rintoul, 2000: Estimates of area-averaged diapycnal fluxes from basin-scale budgets. *J. Phys. Oceanogr.,* **30,** 2320–2341.

——, and ——, 2001a: The Southern Ocean limb of the global deep overturning circulation. *J. Phys. Oceanogr.,* **31,** 143–173.

——, and ——, 2001b: Circulation, renewal, and modification of Antarctic Mode and Intermediate Water. *J. Phys. Oceanogr.,* **31,** 1005–1030.

Spall, M., 2000: Buoyancy-forced circulations around islands and ridges. *J. Mar. Res.,* **58,** 957–982.

Speer, K., S. R. Rintoul, and B. Sloyan, 2000: The diabatic Deacon cell. *J. Phys. Oceanogr.,* **30,** 3212–3222.

Stocker, T., and D. Wright, 1991: Rapid transition of the ocean's deep circulation induced by changes in surface water fluxes. *Nature,* **351,** 729–732.

Stommel, H., 1958: The abyssal circulation. *Deep-Sea Res.,* **5,** 80–82.

Talley, L., 2003: Shallow, intermediate, and deep overturning components of the global heat budget. *J. Phys. Oceanogr.,* **33,** 530–560.

Toggweiler, J. R., and B. Samuels, 1995: Effect of Drake Passage on the global thermohaline circulation. *Deep-Sea Res.,* **42,** 477–500.

Veronis, G., 1973: Model of World Ocean circulation. Part I. *J. Mar. Res.,* **31,** 228–288.

Webb, D. J., and N. Suginohara, 2001: Vertical mixing in the ocean. *Nature,* **409,** 37.

Welander, P., 1959: An advective model of the ocean thermocline. *Tellus,* **11,** 309–318.